Transactions on Engineering Sciences vol 31, © 2001 WIT Press, www.witpress.com, ISSN 1743-3533

# A modified Maxwell stress tensor method for the evaluation of electromagnetic torque

S. Elia[1], M. Pasquali[2], G. Remigi[1], M. V. Sabene[1] & E. Santini[1]
[1] *Dipartimento di Ingegneria Elettrica*
*Università di Roma "La Sapienza", Rome, Italy.*
[2] *Centro Ricerche Enea Casaccia, Rome, Italy.*

## Abstract

This paper shows a new numerical technique for the FEM calculation of the electromagnetic torque in a rotating electric machine. This is an extension of the well-known Maxwell stress tensor method, applied to circular paths that lie entirely in the airgap of rotating machines. Applications allow to evaluate the effectiveness of the method.

## 1 Introduction

There are a number of algorithms that allow numerical evaluation of mechanical forces due to magnetic interactions. They are commonly used in FEM analysis of power devices: [1, 2, 3]:
1. Virtual works;
2. Maxwell stress tensor (MST).

These methods are completely general, and they are not specialized for the evaluation of forces and/or of torques in power devices such as electric machines. It is well known that, from a numerical point of view, both methods are ill-conditioned: the first one because the force is calculated from two field solutions very close the one from the other, the second one because the numerical value of the force depends only on the flux density in the path where the Maxwell tensor is evaluated. On the other hand, integration of the Maxwell tensor along a path (which is 1D in 2D problems and 2D in 3D problems) is not straightforward, and requires very clever programming.

The virtual works method cannot be improved significantly, if not by reformulating the problem, leading thus to the mean and difference potential method [4].

The MST method can be improved by performing an integration which is of the same order as the problem, i.e. 2D for 2D problems, and 3D for 3D problems. This allows one to increase the dimension of the region where the flux density is taken into account when evaluating the MST, reducing the overall error; moreover, integration techniques to be used are standard for that space. Moreover, it will be seen that the evaluation of the torque can be specialized to circular paths.

## 2 Modification of the Maxwell stress tensor method for accurate torque evaluation

With reference to a 2D geometry, the mechanical force $\overline{F}$ acting on a body, due to electromagnetic interaction, has the following components:

$$F_x = \frac{1}{\mu_0}\int_S (\nabla \cdot T_x) dS \qquad F_y = \frac{1}{\mu_0}\int_S (\nabla \cdot T_y) dS \tag{1}$$

In Eq. (1), $S$ is a surface that encompasses the body, and $T_x$ and $T_y$ are :

$$T_x = \vec{i}\left(B_x^2 - \frac{1}{2}|B|^2\right) + \vec{j}B_xB_y \qquad T_x = \vec{i}B_xB_y + \vec{j}\left(B_y^2 - \frac{1}{2}|B|^2\right) \tag{2}$$

where $\vec{i}$ and $\vec{j}$ represent the unit vectors of the coordinate axes.

By applying the divergence theorem to Eqs. (1):

$$F_x = \frac{1}{\mu_0}\int_S (\nabla \cdot T_x) dS = \frac{1}{\mu_0}\int_C T_x \cdot \vec{n} dC \qquad F_y = \frac{1}{\mu_0}\int_S (\nabla \cdot T_y) dS = \frac{1}{\mu_0}\int_C T_y \cdot \vec{n} dC \tag{3}$$

where $C$ is the path that encircles $S$ and $\vec{n}$ is the unit vector of the outward normal to $C$. Since $\vec{n} = \vec{i}\cos\theta + \vec{j}\cos\theta$, Eqs. (3) are rewritten as:

$$F_x = \frac{1}{\mu_0}\int_C \left[\left(B_x^2 - \frac{1}{2}|B|^2\right)\cos\theta + B_xB_y \sin\theta\right] dC \tag{4.a}$$

$$F_y = \frac{1}{\mu_0}\int_C \left[B_xB_y \cos\theta + \left(B_y^2 - \frac{1}{2}|B|^2\right)\sin\theta\right] dC \tag{4.b}$$

Transactions on Engineering Sciences vol 31, © 2001 WIT Press, www.witpress.com, ISSN 1743-3533



With the positions $M = B_x^2 - \frac{1}{2}|B|^2$, $N = B_x B_y$, Eqs. (4) can be rewritten as:

$$F_x = \frac{1}{\mu_0}\int_C [M\cos\theta + N\sin\theta]dC \qquad F_y = \frac{1}{\mu_0}\int_C [N\cos\theta - M\sin\theta]dC \qquad (5)$$

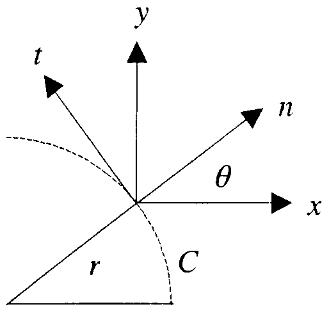


Figure 1: Reference frame for the evaluation of the forces and of the torque ($n$ = normal, $t$ = tangent).

Eqs. (5) can be interpreted as the integral of the elementary force quantities

$$dF_x = \frac{1}{\mu_0}[M\cos\theta + N\sin\theta]dC \qquad dF_y = \frac{1}{\mu_0}[N\cos\theta - M\sin\theta]dC \qquad (6)$$

When dealing with rotating machines, the integration path generally is a circumference $C$ that lies in the airgap and encircles entirely the rotor. Without loss of generality, $C$ can be supposed to have center in the point (0,0) and a radius $r$: the maximum and minimum possible values for $r$ will be denoted $r_1$ and $r_2$ respectively. With these hypotheses, $dC = rd\theta$, and Eqs. (3) are rewritten as:

$$F_x = \frac{1}{\mu_0}\int_0^{2\pi} T_x \cdot \vec{n} r d\theta \qquad F_y = \frac{1}{\mu_0}\int_0^{2\pi} T_y \cdot \vec{n} r d\theta \qquad (7)$$

The elementary numerical value of the torque is (for the conventions of the reference frames, see Fig. 1):

$$dT = rdF_t = r(-dF_x\sin\theta + dF_y\cos\theta) \qquad (8)$$

By introducing into Eq. (8) the expressions for $F_x$ and $F_y$ from Eqs. (5):

Transactions on Engineering Sciences vol 31, © 2001 WIT Press, www.witpress.com, ISSN 1743-3533



$$dT = \frac{r^2}{\mu_0}\left[-\left(M\cos\theta + N\sin\theta\right)\sin\theta + \left(N\cos\theta - M\sin\theta\right)\cos\theta\right]d\theta$$

and the total torque is:

$$T = \int_0^{2\pi} dT = \frac{r^2}{\mu_0}\int_0^{2\pi}\left(N\left(\cos^2\theta - \sin^2\theta\right) - 2M\sin\theta\cos\theta\right)d\theta \tag{9}$$

that can be rewritten as:

$$T = \frac{r^2}{\mu_0}\int_0^{2\pi}\left(N\cos 2\theta - M\sin 2\theta\right)d\theta \tag{10}$$

It has been already underlined that the integration path must lie entirely in the airgap ($r_1 < r < r_2$). From an electromagnetic point of view, the numerical value of integral in Eq. (10) is independent on $r$: if $r$ varies between $r_1$ and $r_2$, the circumference $C$ encircles only different areas of air that, physically, do not contribute to the torque. From a numerical point of view, the numerical value of the rhs of Eq. (10) depends on $r$, due to the rounding and truncation errors in the evaluation of the flux density. With reference to this second viewpoint, lhs of Eq. (10) will be referred at as $T(r)$. More explicitly, $T(r)$ should exhibit the same numerical value for each $r$ that lies completely in the airgap, but numerical errors leads to different numerical values.

It is possible to perform $N$ numerical integrations along $N$ paths at different values of $r$, $r_1 < r < r_2$, equispaced by $\Delta r = (r_2 - r_1) / N$. From an analytical point of view, the torque is the mean value of these $N$ integrals (that, by hypothesis, should have the same value):

$$T = \frac{1}{N}\sum_{i=1}^{N} T(r_i) \tag{11}$$

The rhs can be multiplied by the ratio $(r_2 - r_1) / (r_2 - r_1)$:

$$T = \frac{r_2 - r_1}{r_2 - r_1}\frac{1}{N}\sum_{i=1}^{N} T(r_i) = \frac{1}{r_2 - r_1}\sum_{i=1}^{N} T(r_i)\Delta r \tag{12}$$

If $N$ tends to the infinity, being constant the interval $(r_1, r_2)$:

$$T = \frac{1}{r_2 - r_1} \int_{r_1}^{r_2} T(r)dr = \frac{1}{r_2 - r_1} \frac{1}{\mu_0} \int_{r_1}^{r_2} r^2 \int_0^{2\pi} (N \cos 2\theta - M \sin 2\theta) d\theta dr \tag{13}$$

According to the conventions, cos $\theta = x / r$ and sin $\theta = y / r$. The integral in rhs of Eq. (13) is in the $(r, \theta)$ coordinate system, and it can be changed in the $(x, y)$ coordinate system by considering that, in an annulus:

$$T = \int_{r_1}^{r_2} \int_0^{2\pi} r d\theta dr = \int_S dxdy$$

where $S$ is the annulus defined by $r_1 < r < r_2$. Eq. (13) can be rewritten as:

$$T = \frac{1}{r_2 - r_1} \frac{1}{\mu_0} \int_S \left[ N \left( \frac{x^2}{r} - \frac{y^2}{r} \right) - 2M \frac{xy}{r} \right] dxdy \tag{14}$$

The rhs in Eq. (14) is the expression that leads to the numerical solution of the problem. Due to the summability of the integration, this can be performed piecewise, i.e. triangle by triangle:

$$T = \frac{1}{r_2 - r_1} \frac{1}{\mu_0} \sum_{k=1,N_e} \int_{S_k} \left[ N \left( \frac{x^2}{r} - \frac{y^2}{r} \right) - 2M \frac{xy}{r} \right] dS_k \tag{15}$$

where $N_e$ is the number of (triangular) elements and $S_k$ is the surface of the $k$-th element. It is worth noting that each term of the surface integral in Eq. (15) involves functions of the types $[N\ (x^2 / r)]$, $[N\ (y^2 / r)]$ and $[M\ (xy / r)]$ that, due to the presence of the term $1 / r$, cannot be integrated with the standard techniques used for the formation of [S] and [T] matrices.

The operating differences between the presented algorithm and the conventional ones are easily deduced:

1) In practice, in the proposed method the Maxwell tensor is integrated along a large number of paths rather than along a single path, and the mean value is evaluated. This procedure tends to decrease the approximation errors.
2) The integration domain is of the same order of the main problem. In conventional procedures the integration domain is one order less of the main problem (a line in 2D problems, a surface in 3D problems): this implies the need of specific integration schemes.

## 3 Element integration

The main task in Eq. (15) is the evaluation of the element integral

$$\int_{S_k}\left[N\left(\frac{x^2}{r}-\frac{y^2}{r}\right)-2M\frac{xy}{r}\right]dS_k \tag{16}$$

As already pointed out, this integral cannot be evaluated with standard simplex techniques. Moreover, numerical integration is not straightforward, due to the random position of the triangle in the *xy* reference frame(in 3D, the problem is still greater). It is possible to change a different reference frame, where integration is simpler (from a algorithm point of view).

In the following, a conventional vector potential formulation for FEM analysis of the electromagnetic field is considered, with triangular elements of degree $n$ in $(x,y)$ coordinates. Function in integral in (16) is a polynomial of maximum degree $n + 1$ (apart the factor $1/r$) that, in general, cannot be integrated in a closed form.

Fig. 2 shows one of the triangular elements where integral in (16) must be performed. Without loss of generality, each triangle can be locally renumbered counterclockwise; moreover, it is possible to consider a reference system $(\xi, \eta)$ where the point $(\xi = 0,\ \eta = 0)$ is point 1 of the triangle, and axis $\xi$ is such that point 2 of the triangle has coordinates $(\xi_2, 0)$. A point P, that in the $(\xi, \eta)$ system has coordinates $(\xi_p, \eta_p)$, in $(x, y)$ system has coordinates $(x_p, y_p)$:

$$\begin{vmatrix} x_p \\ y_p \end{vmatrix} = \begin{vmatrix} x_0 \\ y_0 \end{vmatrix} + \begin{vmatrix} \cos\theta & -\sin\theta \\ \sin\theta & \cos\theta \end{vmatrix}\begin{vmatrix} \xi_p \\ \eta_p \end{vmatrix}$$

where $(x_0, y_0)$ are the coordinates in $(x, y)$ system of the origin of $(\xi, \eta)$ reference system, and $\theta$ is the angle between edge $(1 \rightarrow 2)$ of the triangle and axis $x$. It is evident that, descending from the summability of the integration, the element integral can be evaluated as:

$$\int_{S_k} f(x,y)\,dxdy = \int_{S_k} f[x(\xi,\eta), y(\xi,\eta)]\,d\xi d\eta \tag{17}$$

By developing the surface integral:

$$\int_{S_k} f(x,y)\,dxdy = \int_0^{\eta_3}\left[\int_{g_1(\eta)}^{g_2(\eta)} f(x_0+\xi\cos\theta-\eta\sin\theta,\ y_0+\xi\sin\theta+\eta\cos\theta)\,d\xi\right]d\eta \tag{18}$$

where

$$g_1(\eta) = \frac{\xi_3}{\eta_3}\eta \qquad g_2(\eta) = \frac{\eta}{\eta_3}(\xi_3-\xi_2)+\xi$$

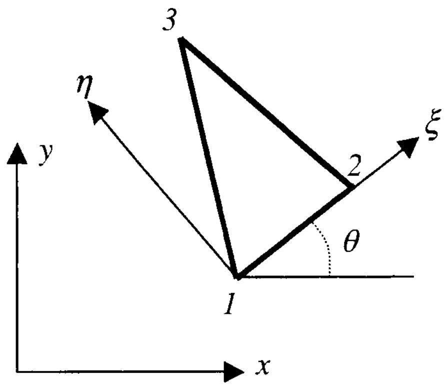


Figure 2: An element in the laboratory frame and the intrinsic reference frame.

From a software point of view, integration of (18) is simpler than (16). A straightforward technique consists in subdividing the (0, $\eta_3$) interval in a number of sub-segments; for each one of these, the inner integrals in (18) are function only of $\xi$ $\xi$ and they can be determined by means of the Cavalieri's rule. A numerical function of $\eta$ is thus deduced, that can be again integrated by means of the same Cavalieri's rule.

## 4 Numerical considerations

The described surface integration is rather different from conventional procedures. It is worth describing some of the results of the numerical investigation.

A 5th order element was taken onto account: in Eq. (18), the maximum power of $\xi$ is 6. A critical triangle was investigated, that presents large values of $\xi$ and small values of $\eta$: the triangle (48,0; 52, 0; 50,3).

Table 1 reports the results of a series of numeric tests. For the element under consideration, the area has been evaluated (i.e. the integral of *1* function). Moreover, the integral of the function ($\xi^6 / r$) was evaluated. It was seen that the said integral depends not only on the number of $\xi$- and $\eta$-divisions, but it also changes for permutation of the indices of the nodes: in column *A* the nodes are taken in the initial sequence (1,2,3), while in columns *B* and *C* they are permuted (this implies that the origin of the ($\xi$ ,$\eta$) reference system changes, as well as the direction of the exes themselves).

As expected, the variation of the integral with the number of divisions and with the numbering of the triangle nodes effect is particularly evident for large values of $\xi$ and for high powers. It is seen in fact that the numerical value of the element area do not changes with the number of elements and the node sequence; the integral of ($\xi^6$ / $r$) is much more sensible to the number of division and to the local numbering of the

Transactions on Engineering Sciences vol 31, © 2001 WIT Press, www.witpress.com, ISSN 1743-3533



nodes. From the numerical results it is, however, evident that the mean value of the integral (i.e. the value obtained by taking the mean between the surface integral in the three possible node sequences) is much closer to the final value.

(123) (123)

Table 1. Numerical value of the integral in Esq. (16) for different value of the sampling nodes for Cavalieri's rule, and for different local numbering of the nodes.

| Number of $\xi$- and $\psi$-divisions | $\int_S d\xi d\eta$ | $\int_S \xi d\xi d\eta$ | A (123) $\int_S \frac{\xi^6}{r} d\xi d\eta$ | B (231) $\int_S \frac{\xi^6}{r} d\xi d\eta$ | C (312) $\int_S \frac{\xi^6}{r} d\xi d\eta$ | $\frac{A+B+C}{3}$ |
|---|---|---|---|---|---|---|
| 2 | 6. | 297.333344 | 1.794913 $10^9$ | 1.922108 $10^9$ | 1.919754 $10^9$ | 1.878925 $10^9$ |
| 4 | 6. | 298.400024 | 1.828179 $10^9$ | 1.904867 $10^9$ | 1.903540 $10^9$ | 1.878862 $10^9$ |
| 6 | 6. | 298.857117 | 1.842656 $10^9$ | 1.896572 $10^9$ | 1.896621 $10^9$ | 1.878616 $10^9$ |
| 8 | 6. | 299.111115 | 1.850757 $10^9$ | 1.893518 $10^9$ | 1.892788 $10^9$ | 1.879021 $10^9$ |
| 10 | 6. | 299.272705 | 1.855934 $10^9$ | 1.890950 $10^9$ | 1.890354 $10^9$ | 1.879079 $10^9$ |
| 12 | 6. | 299.384644 | 1.859528 $10^9$ | 1.889175 $10^9$ | 1.888670 $10^9$ | 1.879124 $10^9$ |
| 14 | 6. | 299.466644 | 1.862169 $10^9$ | 1.887873 $10^9$ | 1.887437 $10^9$ | 1.879160 $10^9$ |
| 16 | 6. | 299.529419 | 1.864191 $10^9$ | 1.886879 $10^9$ | 1.886494 $10^9$ | 1.879188 $10^9$ |
| 18 | 6. | 299.578949 | 1.865789 $10^9$ | 1.886094 $10^9$ | 1.885750 $10^9$ | 1.879211 $10^9$ |
| 20 | 6. | 299.619008 | 1.867084 $10^9$ | 1.885459 $10^9$ | 1.885148 $10^9$ | 1.879230 $10^9$ |
| 2500 | 6. | 299.996826 | 1.879336 $10^9$ | 1.879490 $10^9$ | 1.879486 $10^9$ | 1.879437 $10^9$ |

## 5 Comparison with an exact solution

In order to evaluate the performances of the proposed method, a comparison has been performed between the results of the proposed method and the solution in a case where it is possible to determine the solution in closed form. An electromechanic device was studied, that carries one stator winding and one rotor winding. Both magnetic structures are toothless, and there one slot per pole and per phase (in practice, each conductor has a $\theta$-width equal to one pole pitch).

Assuming the problem to be 2D and linear, the flux density in the airgap can be determined in closed form; the force acting on the conductors (and therefore the machine torque) can be analytically determined, since the torque production mechanism is linked to the Lorentz force. Even if the windings present a thickness in the radial direction, the flux density is purely radial throughout the airgap and the windings.

The analytical behaviour of the flux density, taking into account the variation of the volume of the airgap when the radius changes ( $r_1 \le r \le r_2$) is summarized in Table II, together with the analytical expression of the torque.

The analytical value of the torque has been compared with the results from the proposed method and with the virtual works method. The geometry had the following parameters: $N_sI_s$ = $N_rI_r$ = $18$, $r_1$=$20$, $r_a$ = $20.1$, $r_b$ = $20.4$, $r_2$= $20.5$, $\mu_{fe}$=

Transactions on Engineering Sciences vol 31, © 2001 WIT Press, www.witpress.com, ISSN 1743-3533



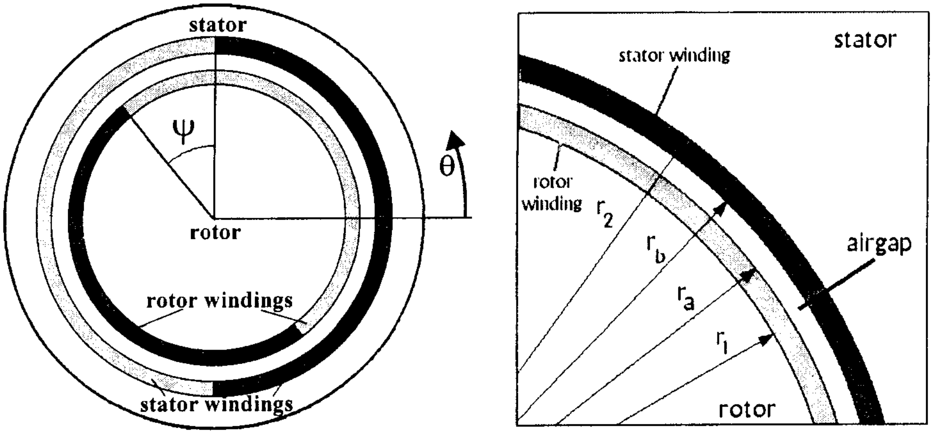


a) b)

Figure 3: a) an electromechanic device for the analytical evaluation of the torque; b) a detail of the airgap region.

Table 2. The analytical behaviour of the flux density and the analytical expression of the torque ($\psi$ is the angle between stator and rotor magnetic axes).

| | $-\frac{\pi}{2} \le \theta \le \frac{\pi}{2}$ | $\frac{\pi}{2} \le \theta \le \frac{3\pi}{2}$ |
|---|---|---|
| $B_r(\theta, r)$ | $\frac{N_r I_r}{\pi} \frac{1}{ln\frac{r_2}{r_1}} \frac{\theta - \psi}{r}$ | $\frac{N_r I_r}{\pi} \frac{1}{ln\frac{r_2}{r_1}} \frac{\pi - \theta + \psi}{r}$ |
| $B_s(\theta, r)$ | $\frac{N_s I_s}{\pi} \frac{1}{ln\frac{r_2}{r_1}} \frac{\theta}{r}$ | $\frac{N_s I_s}{\pi} \frac{1}{ln\frac{r_2}{r_1}} \frac{\pi - \theta}{r}$ |

$$T(\psi) = \frac{N_r N_s I_r I_s}{\pi^2} \frac{(\pi - \psi)\psi}{ln\frac{r_2}{r_1}}$$

*10000.0*, $\mu_{air}$ = *1.0*. Fig. 4 shows the comparison between the analytical results and the numerical results, both from virtual works and from the presented method. There is a substantial agreement between numerical and analytical results, that confirms the reliability and the accuracy of the method.

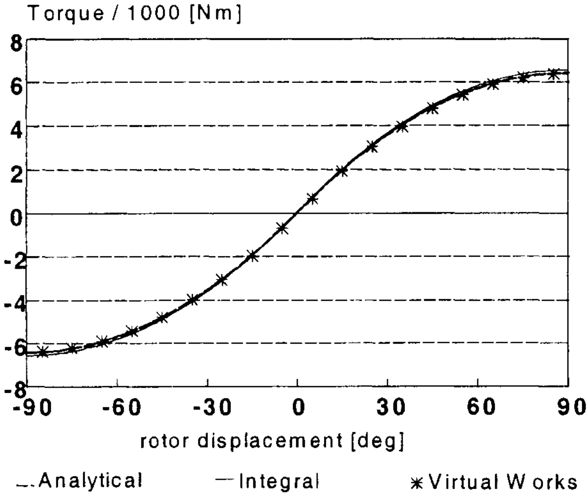


Figure 4: Comparison between the modified Maxwell stress tensor method, the virtual works method and the analytical solution (virtual works: central difference scheme, 10 degrees displacement between the two field solutions).

## 6 Conclusions

The numerical technique described allows accurate evaluation of the electromagnetic torque on a rigid body, starting from FEM results. This is an extension of the well-known Maxwell stress tensor method, applied to circular paths that lie entirely in the airgap. Differently from Maxwell stress tensor, the integral operations related to the numerical calculations are of the same dimension of the FEM problem. A comparison with analytical case confirmed the effectiveness of the method.

## References

[1] E. Santini et al. *FEM Evaluation of Performance of Axial Flux Slotted Permanent Magnet Machines*, IEEE Industry Applications Society, Annual Meeting, St. Louis, Missouri, 12-16 Oct., 1998.

[2] E. Santini et al. *Influence of the Radial Variation of the Magnet Pitch in Slotless Permanent Magnet Axial Flux Motors*, Proceedings of the IEEE/IAS Annual Meeting, 1997.

[3] E. Santini et al. *Numerical Evaluation of Cogging Torque in Slotted Permanent Magnet Axial Flux Machines,* International Symposium on Power Electronics, Industrial Drives, Advanced Machines, Power Quality, (Speedam 98), 3- 5 June 1998, Sorrento (Italy), pp. C3 - 25 to C3 - 30.

[4] Hamdi, E.S., Licariao-Nogueira, A.F. and Silvester, P.P. *Torque Computation by Mean and Difference Potentials,* IEE Proceedings-A, Vol 140, No. 2, March 1993.